FEMS Pathogens and Disease, 74, 2016, ftv111

doi: 10.1093/femspd/ftv111
Advance Access Publication Date: 25 November 2015
Research Article

RESEARCH ARTICLE

Staphylococcus epidermidis: metabolic adaptation and biofilm formation in response to different oxygen concentrations

Cristina Uribe-Alvarez[1], Natalia Chiquete-Félix[1], Martha Contreras-Zentella[2], Sergio Guerrero-Castillo[3], Antonio Peña[1] and Salvador Uribe-Carvajal[1,*]

[1]Department of Molecular Genetics, Instituto de Fisiología Celular, Universidad Nacional Autónoma de México, 04510, México DF, México, [2]Department of Cellular and Developmental Biology, Instituto de Fisiología Celular, Universidad Nacional Autónoma de México, 04510, México DF, México and [3]Nijmegen Center for Mitochondrial Disorders, Radboud University Medical Center, 6525 GA Nijmegen, the Netherlands

*Corresponding author: Department of Molecular Genetics, Instituto de Fisiología Celular, Cdad Universitaria, Apdo Postal 70-472, Coyoacán, 04510 México, México. Tel: +5255-56225632; Fax: +5255-56225630; E-mail: suribe@ifc.unam.mx

One sentence summary: Biofilm formation by Staphylococcus epidermidis is enhanced in anaerobic conditions. Many enzymes are expressed as oxygen becomes low, which can be considered as possible therapeutic targets.

Editor: Tom Coenye

ABSTRACT

Staphylococcus epidermidis has become a major health hazard. It is necessary to study its metabolism and hopefully uncover therapeutic targets. Cultivating *S. epidermidis* at increasing oxygen concentration [O_2] enhanced growth, while inhibiting biofilm formation. Respiratory oxidoreductases were differentially expressed, probably to prevent reactive oxygen species formation. Under aerobiosis, *S. epidermidis* expressed high oxidoreductase activities, including glycerol-3-phosphate dehydrogenase, pyruvate dehydrogenase, ethanol dehydrogenase and succinate dehydrogenase, as well as cytochromes *bo* and *aa3*; while little tendency to form biofilms was observed. Under microaerobiosis, pyruvate dehydrogenase and ethanol dehydrogenase decreased while glycerol-3-phosphate dehydrogenase and succinate dehydrogenase nearly disappeared; cytochrome *bo* was present; anaerobic nitrate reductase activity was observed; biofilm formation increased slightly. Under anaerobiosis, biofilms grew; low ethanol dehydrogenase, pyruvate dehydrogenase and cytochrome *bo* were still present; nitrate dehydrogenase was the main terminal electron acceptor. KCN inhibited the aerobic respiratory chain and increased biofilm formation. In contrast, methylamine inhibited both nitrate reductase and biofilm formation. The correlation between the expression and/or activity or redox enzymes and biofilm-formation activities suggests that these are possible therapeutic targets to erradicate *S. epidermidis*.

Keywords: *Staphylococcus epidermidis*; biofilms; anaerobiosis; pathogenicity; therapeutic target; opportunistic

Received: 11 September 2015; **Accepted:** 23 November 2015

INTRODUCTION

Staphylococcus epidermidis is a coagulase-negative saprophytic inhabitant of the outer skin layers where it excludes pathogenic bacteria such as *S. aureus* (Otto 2009; Cogen *et al.* 2010). Regretfully, when *S. epidermidis* is introduced into tissues by needle punctures or surgical wounds, it becomes a major health hazard as it forms biofilms on catheters or prosthesis forcing their removal (Gristina 1987; Raad, Alrahwan and Rolston 1998). Among coagulase-negative staphylococci-caused prosthetic valve infective endocarditis, *S. epidermidis* is found in 82% cases (Mack *et al.* 2013). Also in 30%–43% implant perioperative infections (Zimmerli, Trampuz and Ochsner 2004) and in 50%–70% catheter-related infections (von Eiff, Peters and Heilmann 2002).

In spite of its growing importance as a human pathogen, the metabolism of *S. epidermidis* has not been fully characterized. Also, the signals that promote biofilm formation are poorly understood, although it is known that stress triggers the expression of proteins that bind cells together and enhance resistance to antiseptics, antibiotics and host defenses (Cramton *et al.* 2001; Vuong and Otto 2002; Kostakioti, Hadjifrangiskou and Hultgren 2013). To optimize treatment, *S. epidermidis* metabolism and biofilm-forming activity have to be understood (Vuong and Otto 2002).

Staphylococcus epidermidis is a facultative anaerobe, i.e. it can survive in a wide range of $[O_2]$. This bacterium thrives on human skin, where $[O_2]$ ranges from 2% to 5% (Peyssonnaux *et al.* 2008) and also in ischemic/anoxic tumors and abscesses where $[O_2]$ is zero (Atkuri *et al.* 2007; Wiese *et al.* 2012). *Staphylococcus epidermidis* biofilm-forming activity increases as $[O_2]$ decreases (Cramton *et al.* 1999, 2001; Cotter, O'Gara and Casey 2009; Cotter *et al.* 2009). Indeed, production of biofilm-associated molecules such as the cell adhesion-promoting, extracellular polysaccharide β-1,6-linked glucosaminoglycan is enhanced at low $[O_2]$ (Cramton *et al.* 1999). Anaerobic growth increases biofilm formation in both *S. aureus* and *S. epidermidis* (Cramton *et al.* 2001; Fuchs *et al.* 2007; Cotter *et al.* 2009).

Bacteria contain branched respiratory chains with multiple terminal oxidases that work at different $[O_2]$ (Anraku 1988). These alternative pathways allow survival in adverse and changing environments (Nakano *et al.* 1997; Mukhopadhyay *et al.* 2002; Gandhi and Chikindas 2007; Desriac *et al.* 2013). In this regard, the closely related *S. aureus* modifies its respiratory chain as $[O_2]$ varies (Taber and Morrison 1964; Artzatbanov and Petrov 1990; Fuchs *et al.* 2007; Gotz and Mayer 2013; Hammer *et al.* 2013). Thus, it was hypothesized that the adaptation of both the response to $[O_2]$ and the propensity to form biofilms are related. The emerging pathological importance of *S. epidermidis* led us to analyze its oxidative phosphorylation machinery as well as the generation of biofilms when grown under aerobic, microaerobic or anaerobic conditions. Such knowledge may uncover different therapeutic targets as it has in other research efforts (Gordon *et al.* 2010; Hurdle *et al.* 2011; Kim *et al.* 2013).

MATERIALS AND METHODS

Materials

Brij 58, Ethylenediaminetetraacetic acid (EDTA), glycerol-3-phosphate, glycerol, horse heart cytochrome c, methyl-viologen, lead (II) nitrate, NAD^+, NADH, ATP, n-dodecyl β-D-maltoside, nitrotetrazolium blue chloride (NBT), phenylmethylsulfonyl fluoride (PMSF), sodium deoxycholate, sodium dithionite, sodium dodecyl sulfate, Gram Stain Kit and trizma base were from Sigma Co (St Louis, MO). Ethanol, magnesium sulfate, potassium nitrate, potassium cyanide, potassium carbonate, potassium hydroxide, sodium phosphate, sodium bicarbonate and succinic acid were from JT Baker (Center Valley, PA). TSB medium, 3,3′-Diaminobenzidine tetrahydrochloride hydrate (DAB) and digitonin were from Fluka (Taufenkirchen, Germany). Ammonium persulfate, acrylamide and Bis N,N′-Methylene-bis-acrylamide were from BioRad (Richmond, CA). Imidazol and ξ-aminocaproic were from MP (Santa Ana, CA). Glucose and ammonium sulfate were from Merck (Kenilworth, NJ); Tryptone was from Difco (Sparks, MD); yeast extract was from Bioxon; and PCR Master mix (2X) was from Thermo Scientific (Whaltham, MA).

Bacterial strain and growth

Staphylococcus epidermidis ATCC 12228 was donated by Dr Juan Carlos Cancino Díaz (Instituto Politécnico Nacional). Bacteria were grown in LB medium at 27°C under aerobic (*Ae*) conditions under shaking (250 rpm) unless otherwise specified; under microaerobic (μA) conditions (5% CO_2 atmosphere, static); and under anaerobic (*An*) conditions generated with GazPak EZ anaerobe pouch in a sealed acrylic chamber (static). Pre-cultures were grown in TSB for 24 h at 37°C, 250 rpm. A 1:15 dilution in LB was made in a sterile 100-well TrueLine Honeycomb Cell Culture Plate and grown at 27°C. Absorbance at 600 nm was measured every 3 h in a Bioscreen C spectrophotometer (Growth Curves, USA). To induce cytochrome *bd* expression, *S. epidermidis* was grown in G-medium (Hanson, Srinivasan and Halvorson 1963) with 0.8% casein hydrolysate, 0.32% L-Glutamic acid, 0.21% D-L alanine and 0.12% asparagine under μA for 48 h (Escamilla *et al.* 1987).

DNA extraction, *mutS* and *yqiL* amplification

DNA extraction was performed with a Quick-gDNA MiniPrep from Zymo Research. *mutS* and *yqiL* genes were amplified by PCR using a PCR Master Mix (Life technologies) containing *Taq* polymerase. Oligonucleotides used to amplifiy a mismatch repair protein *mutS* were as follows:

$$mutS-F3\,(\text{GATATAAGAATAAGGGTTGTGAA}$$
and
$$mutS-R3\;\;\text{GTAATCGTCTCAGTTATCATGTT})$$

which amplified a 412-bp fragment (Thomas *et al.* 2007). Acetyl coenzyme A acetyltransferase *yqiL* oligonucleotides were as follows:

$$yqiL-F2\,(\text{CACGCATAGTATTAGCTGAAG})$$
and
$$yqiL-R2\,(\text{CTAATGCCTTCATCTTGAGAAATAA})$$

which amplified a 416-bp fragment (Wang *et al.* 2003). Both PCR assays involved an initial denaturation at 94°C for 5 min, 35 cycles of 94°C for 1 minute, 55°C for 40 s and 72°C for 40 s; and a final extension of 72°C for 5 min. PCR amplification products were subjected to electrophoresis in 1% agarose gels and ethidium bromide staining.

Biofilm detection

Staphylococcus epidermidis pre-cultures and cultures were performed as indicated previously. After incubation in 300 μL for

6, 12, 24 or 30 h in Costar 96 well plates, each well was gently washed three times with 200 μL phosphate-buffered saline (PBS), dried and stained with 1% crystal violet for 15 min. Plates were rinsed with PBS three more times, and bound crystal violet was solubilized in 200 μL ethanol-acetone (80:20 v/v). Optical density at 600 nm (OD_{600}) was determined in a Polar Star Omega (BMG Labtech) microplate reader (Okajima *et al.* 2006). To evaluate the effect of different respiratory chain inhibitors, cyanide or methylamine was added to the microplate at the beginning of the assay.

Bovine heart mitochondria

Beef heart mitochondria (BHM) obtained as in Löw and Vallin (1963) were a gift from Dr Marietta Tuena (IFC, UNAM). These were used as activity standards for different mitochondrial respiratory enzymes and for ATPase (Wittig, Braun and Schagger 2006; Wittig, Karas and Schagger 2007).

Cell membrane isolation

All procedures were conducted at 4°C. Cells were centrifuged at 10 000 × *g* for 10 min and washed with isolation buffer (50 mM Tris-HCl pH 7.4). The pellet was suspended in isolation buffer plus 1mM EDTA and 1 mM PMSF. Cells were disrupted by five passages through a French Press at 4000 psi (SLM Aminco). The suspension was centrifuged at 10 000 × *g* for 20 min to remove unbroken cells; the supernatant was centrifuged at 200 000 × *g* for 90 min (Niebisch and Bott 2003). The membrane pellet was resuspended and homogenized in isolation buffer plus 1mM PMSF. Protein was quantified by Bradford, frozen at −70°C and stored until further use.

Spectral analysis of cytochromes

Cell membranes from 24-h cultures grown in LB media at 27°C were suspended in 50 mM Tris-HCl buffer (pH 7.4) plus 30% (v/v) glycerol, frozen with liquid nitrogen in 2 mm light path cuvettes and analyzed in an Olis DW2000 spectrophotometer. Differential spectra from 400 to 700 nm were obtained from dithionite-reduced minus persulfate-oxidized and dithionite + CO-reduced minus dithionite-reduced membranes.

Nitrate reductase activity

Cells grown under *Ae*, μ*A* or *An* conditions were sonicated three times 30 s with 10 s rests and centrifuged at 10 000 × *g* for 10 min to remove unbroken cells. Methyl-viologen oxidation by nitrate reductase of the cytosolic membrane extracts was recorded at 546 nm in an Aminco-Olis DW 2000 spectrophotometer. Samples (10 μg protein) were assayed in 50 mM potassium phosphate (pH 7) with 0.2 mM methyl viologen previously reduced with 2.9 mM sodium dithionite. The reaction was started with 5 mM potassium nitrate (Kern and Simon 2009). Specific activities were calculated using an extinction coefficient of 19.5 mM^{-1} cm^{-1}. When indicated, methylamine was added at the beginning of the assay (Franco, Cárdenas and Fernández 1984; McCarty and Bremner 1992).

Electrophoretic techniques and in-gel activities

Clear native gel electrophoresis (CN-PAGE) was performed according to Wittig and Schagger (2005) and Wittig, Karas and Schagger (2007). Isolated membranes from *S. epidermidis* and BHM were solubilized with 1% Brij 58 and 0.5 mg lauryl maltoside/mg protein respectively and shaken for 1 h at 4°C. Membranes were centrifuged at 100 000 × *g* at 4°C for 30 min. Supernatants protein concentration was determined by Bradford and 0.1–0.3 mg protein per well was loaded on 4–12% polyacrylamide gradient gels. When clear native electrophoresis was performed, 0.01% Lauryl maltoside and 0.05% sodium deoxycholate were added to the cathode buffer as in Wittig, Karas and Schagger (2007). Gels were run for an hour at 15 mA/gel in a Bio-rad electrophoresis chamber.

In-gel NADH:NBT oxidoreductase activity (120 μg protein for *S. epidermidis* and 20 μg protein for BHM) was determined by incubating the native gels in 10 mM Tris (pH 7.0), 0.5 mg nitrotetrazolium blue chloride (NBT)/mL and 1 mM NADH. In-gel succinate:NBT oxidoreductase activity (120 μg protein for *S. epidermidis* and 100 μg protein for BHM) was determined by incubating the native gels in 10 mM Tris (pH 7.0), 0.5 mg nitrotetrazolium blue chloride (NBT)/mL and 1 mM succinate. In-gel cytochrome c oxidase activity (150 μg protein for *S. epidermidis* and 20 μg protein for BHM) was determined using diaminobenzidine (Wittig, Karas and Schagger 2007). In-gel ATPase activity (200 μg *S. epidermidis* protein and 100 μg BHM protein) was measured by incubating the CN-gel in 35 mM Tris with 270 mM glycine (pH 8.4) for an hour, then 0.2% $Pb(NO_3)_2$, 14 mM $MgSO_4$ and 8 mM ATP were added (Wittig, Karas and Schagger 2007).

Glycerol-3-phosphate dehydrogenase activity

Activity was measured in lysates from cells grown in different $[O_2]$ in fresh 33 mM ammonium sulfate, 100 mM carbonate-bicarbonate buffer, 1 mM NAD^+ (pH 7.0) and 100 mM of glycerol-3-phosphate as substrate. Final solution was adjusted to pH 9.0 with KOH or HCl. Absorbance change for NADH was measured at 340 nm and specific activities were calculated (Burton 1955; Van Eys, Nuenke and Patterson 1959).

Mass spectrometry

From the CN-PAGE gel, the indicated bands were excised and in-gel digested with trypsin. Peptides were analyzed by liquid chromatography tandem mass spectrometry (LC-MS/MS) a in a Q-exactive mass spectrometer (Thermo Fisher Scientific) equipped at the front end with a nano-flow high-performance liquid chromatography system Agilent1200s (Wessels *et al.* 2013). Peptides were separated in a 100 μm ID PicoTip emitter column filled with 3 μm C18 reverse phase silica beads using 30 min linear gradients of 5%–35% acetonitrile with 0.1% formic acid. The mass spectrometer operated in a Top 20 dependent, positive ion mode switching automatically between MS and MS/MS. Full scan MS mode (400–1400 m z^{-1}) was operated at a resolution of 70 000 with automatic gain control target of 1 × 10^6 ions and a maximum ion transfer of 20 ms. Raw files were analyzed by MaxQuant software (version 1.5). Spectra were searched against the *S. epidermidis* database with additional sequences of known contaminants and reverse decoy with a strict FDR of 0.01. Trypsin was selected as the protease with two missed cleavages allowed. Dynamic modifications included N-terminal acetylation and oxidation of methionine. Cystein carbamidomethylation was set as fixed modification.

Oxymetry

Staphylococcus epidermidis grown under *Ae*, μ*A* or *An* conditions were resuspended in 10 mM Hepes pH 7.4. Protein

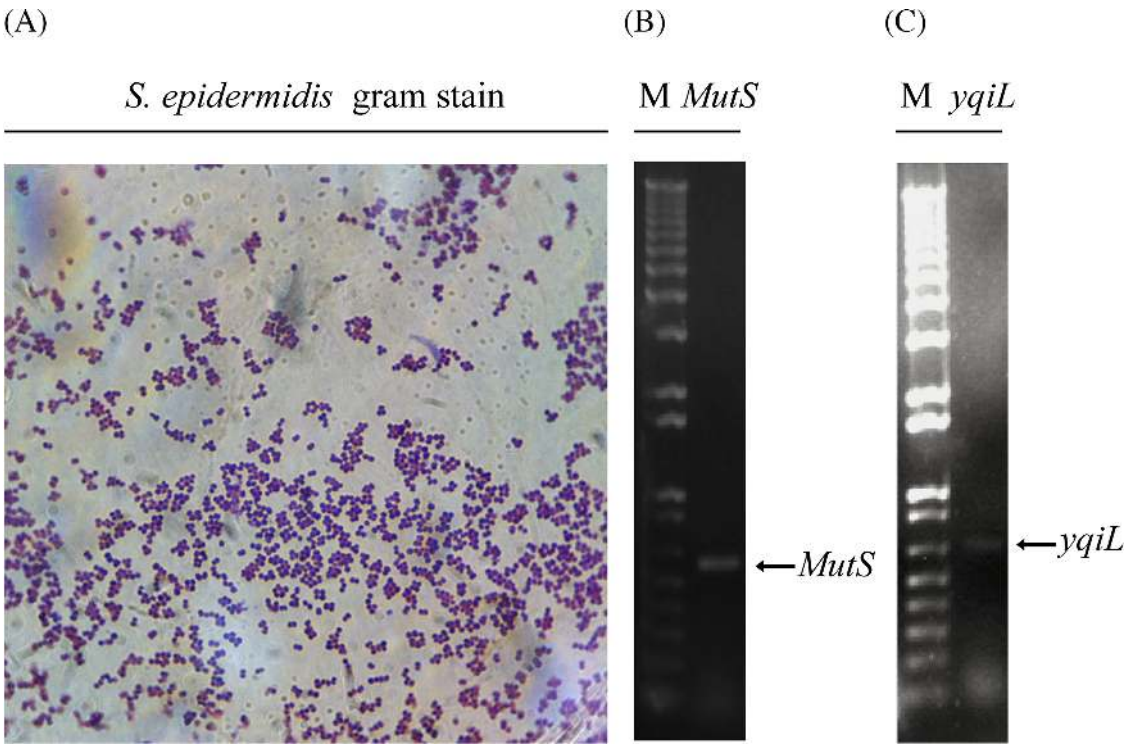

Figure 1. Characterization of *S. epidermidis* ATCC 12228. (**A**) Gram stain was performed using a kit from Sigma diagnostics HT90-A. Image shows Gram-positive cocci in clusters, diplococci and cocci. (**B**) Staphylococcus *epidermidis*-specific gene amplification. 1: 1kb plus marker, Invitrogen. 2: PCR product of DNA mismatch repair protein oligonucleotides (mutS) of 412 pb C. Staphylococcus *epidermidis* specific gene amplification. 1: 1kb plus marker, Invitrogen. 2: PCR product of Acetyl coenzyme A acetyltransferase (yqiL) of 416 pb.

concentration was determined by Biuret in a Beckman Coulter spectrophotometer at 540 nm. Oxygen consumption by cells was assessed in an oxygen meter model 782 (Warner/Strathkelvin Instruments) with a Clark type electrode in a 1 mL water-jacketed chamber at 30°C. Approximately 5 mg mL^{-1} of cells were added to the chamber. Reaction was started by the addition of 10 μM of ethanol (Guerrero-Castillo *et al.* 2009). Data were analyzed using the 782 Oxygen System Software (Warner/Strathkelvin Instruments). Different concentrations of cyanide were used as a respiratory chain inhibitor in order to block oxygen consumption.

Statistics

Results are expressed as mean ± standard deviation from at least four individual experiments to which Tukey´s test was applied. Significance levels and number of experiments were specified under each figure.

RESULTS

Staphylococcus epidermidis adaptability to different [O_2] is illustrated by the plasticity of the respiratory chain and the variations in biofilm formation. Under the microscope, *S. epidermidis* ATCC 12228 colonies formed typical clusters (Fig. 1A). The identity of *S. epidermidis* ATCC 12228 was confirmed by amplifying DNA oligonucleotides from the mismatch repair protein (*mutS*) (Fig. 1B, first gel) and from acetyl coenzyme A acetyltransferase (*yqiL*) (Fig. 1B, second gel). (Wang *et al.* 2003; Thomas *et al.* 2007)

Bacterial growth and biofilm formation at different [O_2]. The adaptability of *S. epidermidis* to different [O_2] was analyzed in cultures under atmospheric oxygen, with (*Ae*) or without agitation, under μ*A* or under *An* conditions (Fig. 2A). In the absence of agitation, at all [O_2] tested, cells grew to a similar density reaching the stationary phase at 24–27 h. In contrast, under agitation at atmospheric [O_2] (*Ae*) the stationary phase was reached within half the time (Fig. 2A).

Even though *S. epidermidis* ATCC 12228 is considered a low-virulence, low-biofilm forming strain, we were able to detect biofilm formation (Fazly Bazzaz *et al.* 2014). In this strain, biofilm-generation decreased as [O_2] increased (Fig. 2B). In *Ae* cells with agitation, biofilms were hardly detectable and they increased slightly in cells subjected to *Ae*-without shaking. Biofilms were large in μ*A* and *An* samples (Fig. 2B). Thus, in *S. epidermidis* increasing [O_2] stimulated growth while inhibiting biofilm formation. i.e. at low oxygen concentration, biofilm formation was high, suggesting that low [O_2] contributes to bacterial virulence (Gristina 1987; Raad, Alrahwan and Rolston 1998).

Detection of Oxidative Phosphorylation-related proteins in S. epidermidis grown at different [O_2]. The adaptive response of *S. epidermidis* to different [O_2] implies handling [O_2] and phosphorylating ADP. Thus, we evaluated the composition of the respiratory chain and the expression of F_1F_0-ATPase. Solubilized plasma membranes from *Ae*, μ*A* or *An* cells were subjected to clear native PAGE, and protein bands were revealed by Coomassie blue staining (Fig. 3A). These samples were used to measure in-gel NADH dehydrogenase (Fig. 3B), succinate dehydrogenase (Fig. 3C) and ATPase (Fig. 3D) activities. In all cases, BHM were used as a positive control (Fig. 3 BHM lanes). BHM bands were labeled according to the migration and activity patterns reported for each complex (I, V, III, IV and II) (Fig. 3A BHM) (Schagger and von Jagow 1991; Wittig, Braun and Schagger 2006; Wittig, Karas and Schagger 2007). I for NADH dehydrogenase activity from complex I, V for ATPase activity of complex V and II for succinate dehydrogenase activity of complex II. Bands corresponding to

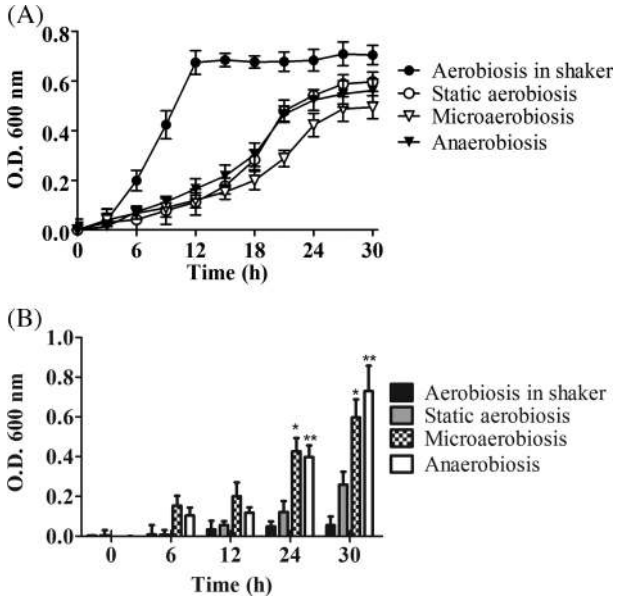

Figure 2. *Staphylococcus epidermidis* growth and biofilm formation under different aeration conditions. (**A**) Growth curves of *S. epidermidis* at 27°C at aerobic (atmosphere oxygen level) with and without shaking, microaerobic (5% CO_2) and anaerobic environment. Absorption at 600 nm was measured in a Bioscreen C spectrophotometer. Data shown are mean ± S.D. from $n = 18$. (**B**) Staphylococcus *epidermidis* biofilm formation at 6, 12, 24 or 30 h. Solubilized crystal violet was measured at 600 nm using a Polar Star Omega (BMG Labtech) microplate reader. Tukey´s comparison test showed significant difference ($^*P < 0.05$) between biofilm formation in microaerobic and anaerobic conditions between 6 and 24 and 30 h. After 6 h, a significant biofilm formation difference ($^*P < 0.05$) was found between aerobic conditions with and without shaking and microaerobic and anaerobic conditions. No difference was observed between oxygen-limited conditions at all times, $n = 6$.

BHM respiratory complexes III and IV are also indicated although no complex III or IV activities were detected in *S. epidermidis* (result not shown). *Staphylococcus epidermidis* cells grown at different [O_2] exhibited different protein bands (Fig. 3A, *S. epidermidis* lanes) that were further analyzed for oxidoreductase and ATPase activities.

NADH dehydrogenase in-gel activity (Fig. 3B) in BHM complex I was detected at 1000 kDa NADH dehydrogenase activity band (Fig. 3B, BHM band I) (Wittig, Braun and Schagger 2006; Wittig, Karas and Schagger 2007). For *S. epidermidis* grown in *Ae*, four NADH dehydrogenase activity bands of lower molecular weight were observed (Fig. 3B lane *S. epidermidis Ae*). In *μA* or *An* cells, these bands were either not observed (N1) or were much lighter (N2, N3 and N4) (Fig. 3B, lanes *S. epidermidis Ae*, *μA* and *An*).

Complex II succinate dehydrogenase activity from BHM was detected as a single 130 kDa band (Fig. 3C, BHM, band II) (Wittig, Braun and Schagger 2006). In *S. epidermidis*, one succinate dehydrogenase activity band was detected in *Ae* grown cells and was practically lost under O_2-limiting conditions (Fig. 3A and C, lanes *S. epidermidis Ae*, *μA* and *An*).

Cytochrome c oxidase in-gel activity was detected in BHM membranes as a single band (results not shown) corresponding to complex IV, MW 200 kDa (Wittig, Braun and Schagger 2006). No oxidase activity was detected in *S. epidermidis* even when adding up to 300 *μ*g of protein (results not shown). Thus, in agreement with others (Taber and Morrison 1964), it is concluded that cytochrome c oxidase is not present in *S. epidermidis*.

The ATPase activity assay revealed a strong band in the BHM sample (Fig. 3D, BHM, band V). *Staphylococcus epidermidis Ae* exhibited two ATPase activity bands (Fig. 3D, *Ae*, bands A1 and A2 while *μA* and *An* revealed only one band (Fig. 3D *μA* and *An* bands). Taken together, the above data indicate that in *S. epidermidis* oxidative-phosphorylation-related activities increased in cells grown at higher [O_2].

Identification of in-gel activity bands by mass spectroscopy: Bands exhibiting the tested oxidoreductase or ATPase activities (Fig. 3), i.e. bands N1, N2, N3, N4, S1 and A1 were identified by LC-MS/MS and were matched against all *S. epidermidis* protein entries of the NCBI database (Table 1). Band N1 sequencing revealed, among other proteins, an aerobic glycerol-3-phosphate dehydrogenase, a NADH dehydrogenase-like protein (SE_0635) and a glycine decarboxylase complex. Band N2 contained the pyruvate dehydrogenase complex (PDC), constituted by

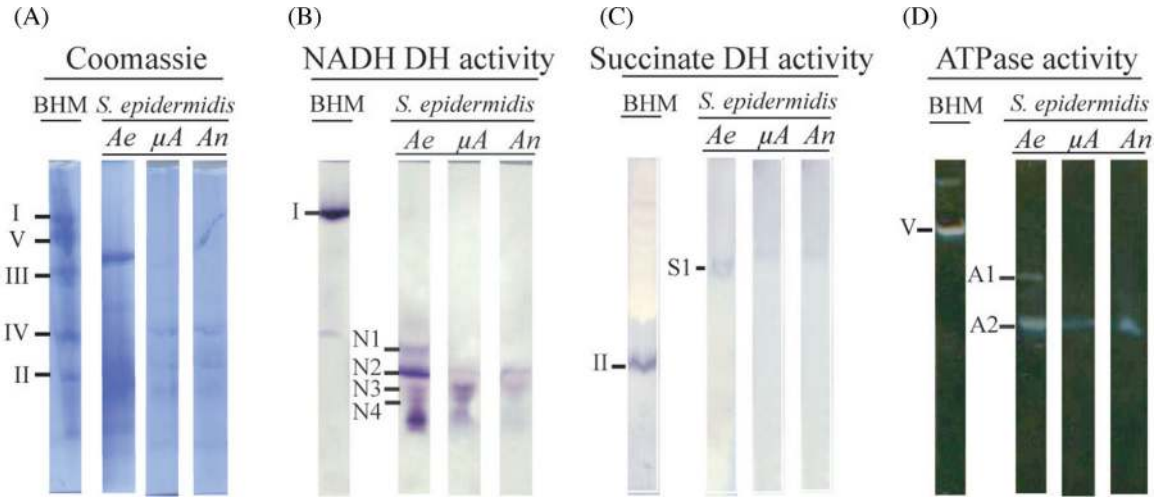

Figure 3. *Staphylococcus epidermidis* membrane protein electrophoretic analysis. Oxidoreductase in-gel activities from *S. epidermidis* membranes grown in different [O_2] were evaluated. BHM was solubilized with Lauryl maltoside. Staphylococcus *epidermidis* membranes were obtained from cultures grown under: (*Ae*) aerobic conditions, (*μA*) microaerobic conditions, (*An*) anaerobic conditions. (**A**) Solubilisates were resolved by CN-PAGE in a 4%–12% polyacrylamide gradient gel and stained with Coomasie. (**B**) In-gel NADH-NBT activity: BHM revealed complex I band (**I**) and *S. epidermidis* aerobic grown membranes revealed four bands labeled as N1, N2, N3 and N4. (**C**) In-gel Succinate-NBT activity: BHM band II corresponds to complex II. Band S1 of *S. epidermidis* was present only in aerobic growth conditions. (**D**) In-gel ATPase activity: BHM Band V corresponds to complex V. *S. epidermidis* ATPase activity was labeled as bands A1 and A2.

Table 1. Analyzed proteins by LC/MS-MS protein sequencing from a Coomassie stained CN-PAGE gel.

Band	Protein name or BLAST homology	NCBI database number	Peptides	MW (kDa)	PEP
N1	Aerobic glycerol-3-phosphate dehydrogenase (*S. epidermidis* ATCC 12228)	gi|81842889	27	62.3	4.62^{-211}
	NADH dehydrogenase-like protein SE_0635	gi|695605246	3	43.86	2.02^{-10}
	Glycine decarboxylase subunit 1	gi|81674491	6	49.96	5.8^{-48}
	Glycine decarboxylase subunit 2	gi|81674492	4	56.4	5.72^{-11}
N2	Dihydrolipoamide dehydrogenase (E3)	gi|721492590	21	49.7	0
	Pyruvate dehydrogenase E1 component subunit β	gi|81674992	21	35.29	1.07^{-167}
	Pyruvate dehydrogenase E1 component subunit α	gi|81674993	12	41.33	1.63^{-222}
	Dihydrolipoamide acetyltransferase component (E2)	gi|694237422	10	46.22	1.08^{-52}
	Glycerol-3-phosphate dehydrogenase	gi|81674534	19	36.12	6.54^{-36}
	Malate:quinone oxidoreductase	gi|721493807	9	56.35	2.51^{-29}
N3	Dihydrolipoamide dehydrogenase	gi|721492590	21	49.7	0
	NADH dehydrogenase-like protein SE_0635	gi|695605246	5	43.86	1.35^{-16}
	Lactate dehydrogenase, partial	gi|520977789	3	32.54	5.04^{-11}
N4	Alcohol dehydrogenase	gi|721493754	13	37.8	9.40^{-225}
	Glyceraldehyde-3-phosphate dehydrogenase	gi|81675183	7	36.2	3.96^{-57}
	Lactate dehydrogenase, partial	gi|520977789	3	36.19	3.39^{-25}
S1	Succinate dehydrogenase/fumarate reductase, flavoprotein subunit	gi|721492636	29	65.631	9.83^{-102}
	Succinate dehydrogenase	gi|721492637	9	31.43	0
	Putative succinate dehydrogenase, cytochrome *b*556 subunit	gi|291319172	1	20.2	6.22^{-8}
	cytochrome *aa3* quinol oxidase, subunit I (*S. caprae*)	gi|242348990	10	75.38	$1.37E^{-97}$
	cytochrome *aa3* quinol oxidase, subunit II (*S. caprae*)	gi|242348991	7	42.7	$6.04E^{-76}$
A1	ATP synthase subunit alfa	gi|81170377	22	54.7	0
	ATP synthase subunit beta	gi|81170379	35	55.6	0
	ATP synthase subunit delta	gi|488441919	11	16.8	5.52^{-147}
	ATP synthase subunit gamma	gi|81842668	10	31.94	2.68^{-97}
	ATP synthase F1, epsilon subunit	gi|691218402	4	14.09	3.48^{-73}
	ATP synthase subunit b	gi|81842667	3	19.47	1.07^{-26}

pyruvate dehydrogenase, dihydrolipoamide acetyltranferase and dihydrolipoamide dehydrogenase, a glycerol-3-phosphate dehydrogenase, and a malate:quinone oxidoreductase; band N3 also contained enzymes from the PDC, a partial lactate dehydrogenase (LDH) and the NADH dehydrogenase-like protein (SE_0635) found in the N1 band; in N4 proteins included alcohol dehydrogenase, glyceraldehyde-3-phosphate dehydrogenase, a partial LDH (Table 1). Aerobic glycerol-3-phosphate dehydrogenase (SE_0979 MW = 62.3 kDa) from the N1 band is the one with highest number of peptides identified and the least error. Previous work in isolating glycerol-3-phosphate dehydrogenase from Escherichia *coli* (Schryvers, Lohmeier and Weiner 1978) and data from the crystal structure (Yeh, Chinte and Du 2008) indicate that the aerobic glycerol-3-phosphate dehydrogenase works as a dimeric enzyme, so it is possible that in *S. epidermidis* glycerol-3-phosphate dehydrogenase is also a dimer that feeds electrons directly to the respiratory chain. NADH dehydrogenase-like protein (SE_0635 MW = 43.86 kDa identified in bands N1 and N3 with a very low peptide count and a high posterior error (PEP) may be a type 2 NADH:quinone oxidoreductase (NDH-2), which is a single 50 kDa subunit protein with FAD as a non-covalently bound cofactor (Schurig-Briccio *et al*. 2014). Bacterial complex I weighs 500–600 kDa depending on the bacterium under study (Young, Jaworowski and Poulis 1978; Young *et al*. 1982; Bergsma, Van Dongen and Konings 2008; Baradaran *et al*. 2013). The *S. epidermidis* genome shows no other NADH dehydrogenases (NC_004461.1). As reported for *S. aureus* (Schryvers, Lohmeier and Weiner 1978), bacterial respiratory complex I was absent in *S. epidermidis*. Unrelated to oxidoreductase activity, we found glycine decarboxylase, a membrane-bound complex that catalyzes the oxidative decarboxylation of glycine.

Both N2 and N3 bands (Table 1) contain the PDC. PDC contains multiple copies of all three enzymatic components: pyruvate dehydrogenase E1 components α (Q8CPN3) and β (Q8CPN2) and dihydrolipoamide acetyltransferase E2 (Q8CTW0), and dihydrolipoamide dehydrogenase E3 (GenBank: KGY36148.1). The PDC decarboxylates pyruvate into acetyl-CoA that participates in the citric acid cycle and feeds the electron transport chain. Band N2 also revealed a malate:quinone oxidoreductase. The malate:quinone oxidoreductase complex oxidizes malate to oxaloacetate donating its electrons to quinone. This complex is absent in mammalians, which makes it a potential drug target. Bands N3 and N4 revealed the presence of an LDH. LDH from *Lactobacillus casei* is a dimeric 70 kDa enzyme (Padgaonkar and Nadkarni 1980). Finally, band N4 has an alcohol dehydrogenase, reported to be a dimeric enzyme of approximately 80 kDa (Hammes-Schiffer and Benkovic 2006).

Band S1 sequence revealed a succinate dehydrogenase/fumarate reductase flavoprotein subunit (SE_0841, MW = 66 kDa). The much larger mass observed here suggests that we isolated the whole succinate dehydrogenase complex (SDC), including succinate dehydrogenase cytochrome *b*-558 (SE_0840, MW 23.67 kDa) and succinate dehydrogenase iron–sulfur protein subunit (SE_0842, MW 31.4 kDa). The complex may also be interacting with other proteins. In *Bacillus subtilis*, the CN-PAGE in-gel activity band for succinate dehydrogenase is reported at 301 kDa because a complex with nitrate reductase may be formed (Sousa *et al.* 2013). In *Wolinella succinogenes* and in *E. coli*, the SDC is crystallized as a dimeric enzyme (Lancaster and Kroger 2000; Cecchini *et al.* 2002). Also, SDC might be in a complex with one or two small hydrophobic polypeptides that anchor the enzyme to the membrane and are required for electron transfer to quinone (Hederstedt 1980, 1986). In band S1, an additional cytochrome *aa3* quinol oxidase was found.

No activity was found when trying to measure in-gel activities with cytochrome *c* as electron donor, which was expected as electrons are donned directly from ubiquinol to oxidases.

The A1 band was F_1F_0-ATPase as confirmed by finding F_1 subunits alfa, beta, delta, gamma and epsilon, plus the F_0 subunit b (Table 1). The number of bands detected may vary depending on the detergent, although the *Ae* grown cells have stronger bands and probably more activity. Comparison with the literature indicates that digitonin-solubilized *B. subtilis* membranes contained three ATPase activity bands at MW = 487, 277 and 187 kDa. (Sousa *et al.* 2013).

Glycerol-3-phosphate dehydrogenase activity. Aerobic glycerol-3-phosphate dehydrogenase was identified as the most prominent protein in band N1, and in-gel activities indicate that it is highly inhibited as $[O_2]$ decreases. Thus, we decided to test its activity in extracts from *S. epidermidis* grown at different $[O_2]$ (Fig. 4). As expected, glycerol-3-phosphate dehydrogenase activity was much higher in *Ae* grown cells and decreased dramatically in under oxygen-limiting conditions (Fig. 4).

The respiratory chain terminal oxidases from S. epidermidis are differentially expressed at different $[O_2]$. In order to increase our understanding of the adaptability of *S. epidermidis* to $[O_2]$, it was decided to analyze the terminal electron acceptors in the respiratory chain, considering that, while the different O_2-dependent oxidases reduce O_2, anaerobic respiratory chains contain enzymes that use fumarate, nitrite, nitrate or DMSO as final electron acceptors (Haddock and Jones 1977).

Differential absorbance spectra of membrane extracts obtained at 77 K indicated that in the respiratory chain from *S. epidermidis* grown at different $[O_2]$, *b*-type cytochrome peaks were observed at 426–427 nm and 555–557 nm; *a*-type cytochromes

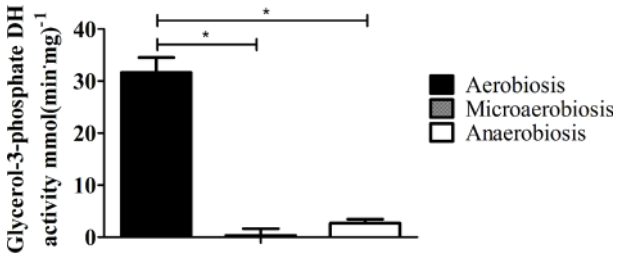

Figure 4. Glycerol-3-phosphate dehydrogenase activities from *S. epidermidis* grown at different oxygen concentrations. NADH absorbance change was measured at 340 nm and specific activities were calculated for extracts from *Ae*, μ*A* and *An* cells. Glycerol-3-phoshate dehydrogenase activity was much higher in aerobic cell growth conditions than in oxygen-limited growth conditions. Tukey's comparison test showed G-3-PDH activity difference between the aerobic and microaerobic grown cells and aerobic and anaerobic grown cells. Significance is $^*P < 0.05$.

were observed as a shoulder at 441–451 and peak at 604 nm. The absence of a peak at 630 nm in all samples is indicative of the lack of a *d*-type cytochrome. The absence of shoulders at 417 and 550 nm indicates the lack of *c*-cytochromes (Fig. 5). When $[O_2]$ was restricted, i.e. at μ*A* or *An*, complete loss of *a*-type cytochromes (*aa3*) (shoulders at 441 and 451 nm and peak at 604 nm) and a decrease in *b*-type cytochromes were observed (peaks at 427 and 557 nm) (Fig. 5). The detection of a small amount of cytochrome *b* in the anaerobic sample is in contrast with a report where complete loss of cytochromes was observed in *S. epidermidis* grown in anaerobic conditions for 16 h (Jacobs and Conti 1965) and in agreement with Frerman and White (1967) where the presence of cytochromes *b* and *o* is reported. The lack of cytochrome *c* confirmed the absence of cytochrome oxidase and in turn, the lack of cytochromes *d* confirmed the absence of *bd*-cytochromes (Fig. 5) as has been reported by others (Taber and Morrison 1964).

To further analyze the respiratory chain terminal oxidases from *S. epidermidis* grown at different $[O_2]$, CO-dithionite-reduced minus dithionite-reduced difference spectra were obtained from *Ae* or μ*A* membranes (Fig. 6) These spectra have an absorbance maximum at 417 nm, and smaller peaks at 545 and 575 nm together with valleys at 430 and 554 nm which are indicative of presence of a CO complex with cytochrome *o* (Fig. 6). Thus, it may be concluded that cytochrome *bo* was present in both *Ae* and μ*A S. epidermidis* (Frerman and White 1967)

Although *S. aureus* and *S. epidermidis* have *cydAB* genes, cyt *bd* has not been found by spectroscopy (Taber and Morrison 1964; Jacobs and Conti 1965). This may be due to an insufficient expression of *cydAB* genes. In all cases only *b*-type cytochromes were observed (Fig 6). In *S. epidermidis* cytochrome *d* was absent in μ*A* cells (Fig. 6) or in those grown in the presence of KCN (results not shown). Thus, in *S. epidermidis* both μ*A* and *Ae* cells express *o*-type cytochromes, while an *a*-type cytochrome was expressed in *Ae* cells.

Staphylococcus epidermidis grown under anaerobic conditions increases expression of nitrate reductase. Anaerobically grown *S. epidermidis* expresses nitrate reductase (Kucera, Dadak and Dobry 1983). In our hands, nitrate reductase activity in *An* was 0.215 ± 0.017 mmol(min·mg)$^{-1}$ protein. Then, in μ*A* it decreased to 0.085 ± 0.01 mmol(min·mg)$^{-1}$ protein. In *Ae* cells, nitrate reductase activity decreased further, to 0.015 ± 0.012 mmol(min·mg)$^{-1}$ protein, 14 times less than in *An* (Fig. 7). Thus, when under *An*, *S. epidermidis* expressed nitrate reductase to substitute oxygen with nitrate as a terminal electron acceptor.

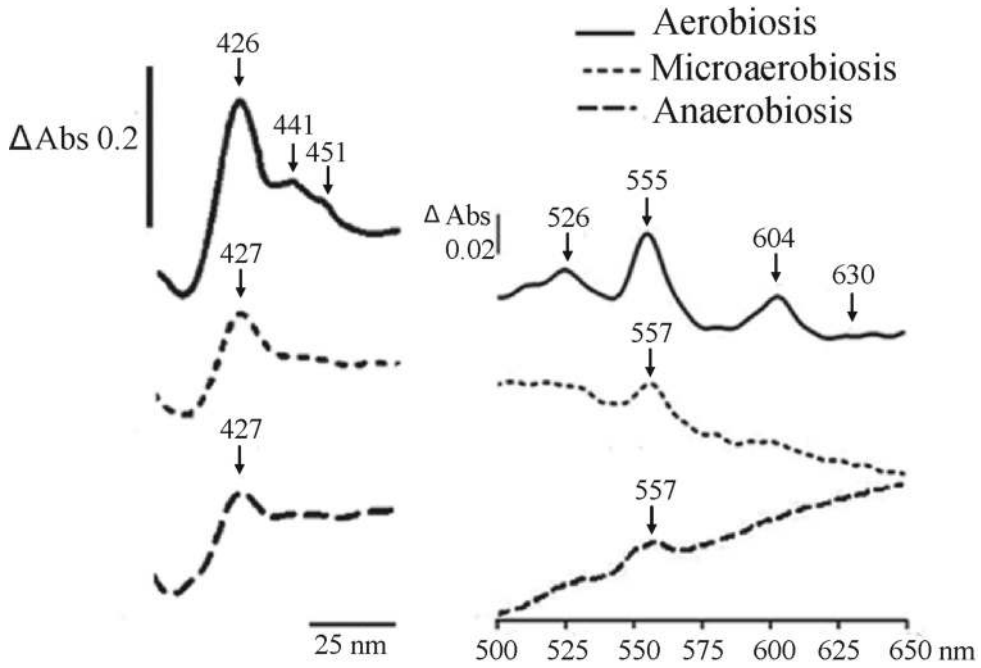

Figure 5. Difference spectra (dithionite-reduced minus persulfate-oxidized) of membranes from cells cultured under different [O_2]: (——) *Ae*, (- - -) μ*A*, (– – –) *An*. Spectra were recorded at 77 K. Membrane protein from 24 h-grown cells in LB medium were adjusted to 15 mg/ml. *b*-type cytochromes can be observed at 426–427 nm and at 555–557 nm in all conditions, *a*-type cytochromes can be observed as a shoulder at 441–451 and peak at 604 nm in membranes obtained from aerobic grown cells. In all samples, *c*-cytochrome shoulders at 417 and 550 nm are absent as well as the *d*-type cytochrome peak at 630 nm.

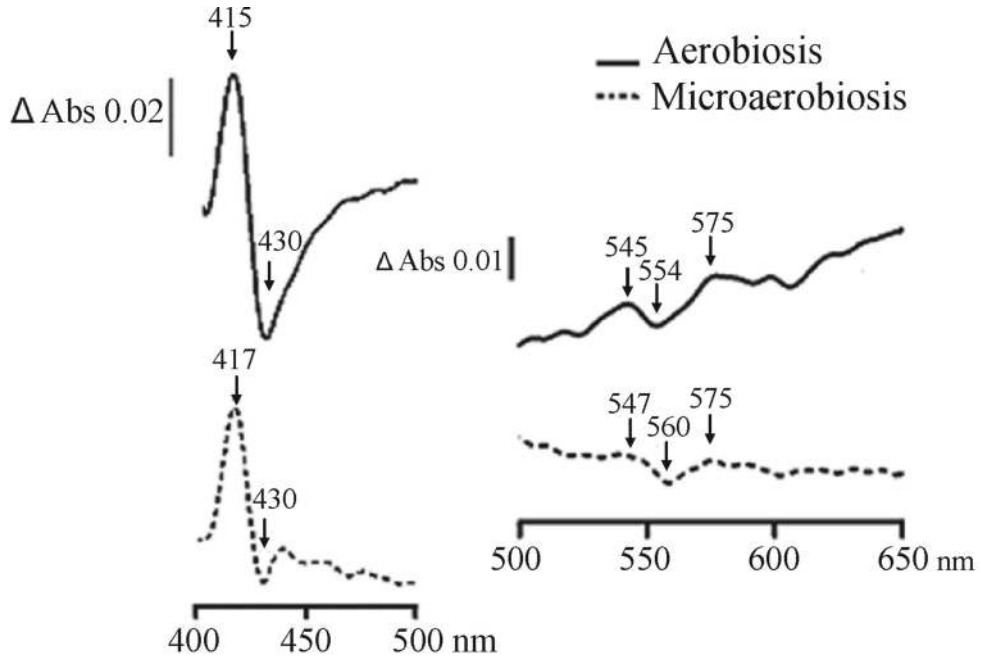

Figure 6. CO Difference spectra (CO + dithionite-reduced minus dithionite-reduced) of membranes from cells cultured under different conditions: (——) *Ae*, (- - -) μ*A*, (– – –) *An*. Spectra were recorded at 77 K. Membrane protein from 24 h grown cells in LB medium were adjusted to 15 mg/ml. A CO complex resembling that of cytochrome o with the Söret peak at 417 nm and peaks at 545 and 575 nm and troughs at 430 and 560–554 nm can be observed. In both conditions, there is a small peak at 592 nm with a shoulder at 445 indicating the presence of an a-type cytochrome.

Cyanide inhibits oxygen consumption and promotes biofilm formation in S. epidermidis. After evaluating the respiratory chain electron acceptors available, we decided to test if mimicking an anaerobic environment by inhibiting the cytochromes *aa3* and *bo* with cyanide would increase biofilm formation. Oxygen consumption in aerobic cells was completely inhibited with 200 μM of cyanide (Fig. 8A). Then biofilm formation was evaluated in the same concentrations of cyanide in cultures grown to 24 or 30 h. At 24 h biofilm formation promotion by cyanide was suggested but not clear. However, at 30 h we observed an increase in the biofilm formation as we exposed *S. epidermidis* to increasing concentrations of cyanide reaching 0.50 ± 0.04 which is close to the

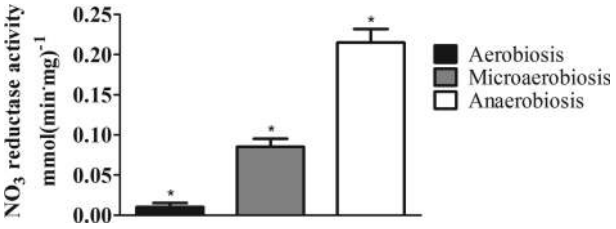

Figure 7. Nitrate reductase activity of *S. epidermidis* grown at different oxygen concentrations. Nitrate reductase activity was measured by means of methylviologen oxidation, which was previously reduced by 2.9 mM of sodium dithionite. Reaction was monitored at 546 nm. Data shown are mean ± S.D. from $n = 4$. Tukey´s comparison test showed significant differences (*$P < 0.05$) between all conditions.

0.59 ± 0.09 obtained in microaerobic conditions. At 24 h, no significant differences in biofilm formation were observed (Fig. 8B).

Methylamine inhibits nitrate reductase activity and biofilm formation in S. epidermidis ATCC 12228. Methylamine is reported to inhibit nitrate reductase activity at 150 mM. We measured nitrate reductase of *S. epidermidis* grown in microaerobic conditions using different concentrations of methylamine (Fig. 8C) and found that at 10 mM methylamine nitrate reductase activity was fully inhibited. Afterwards, biofilm formation was evaluated in cells grown in microaerobic conditions and in the presence of different methylamine concentrations and a decrease in biofilm formation was observed at (Fig. 8D). Microaerobic conditions were used and not anaerobic conditions, because under anaerobic conditions bacteria would be unable to grow (result not shown). This is explained by the lack of oxygen for cytochromes and the inhibition of nitrate reductase.

As *S. epidermidis* gains pathogenic importance it becomes necessary to study its metabolic adaptations to different environmental conditions. Our results provide an image of the plasticity of the *S. epidermidis* respiratory chain. Branched respiratory chains from pathogens may contain therapeutic targets. For instance, *S. epidermidis* expresses an MQO complex, a *bo* cytochrome and a nitrate reductase not found in mammals. Several known inhibitors of *bo* cytochrome (Meunier *et al.* 1995) and nitrate reductase (Magalon *et al.* 1998; Moreno-Vivian *et al.* 1999; Gates *et al.* 2003) might prevent *S. epidermidis* colonization of tissues or prosthetic devices.

DISCUSSION

O_2 is the final electron acceptor in aerobic oxidative phosphorylation, which is the main source of ATP. Bacteria sense substrates and environmental conditions adjusting their metabolism to optimize ATP yields and minimize production of toxic O_2 partial-reduction molecules known collectively as reactive oxygen

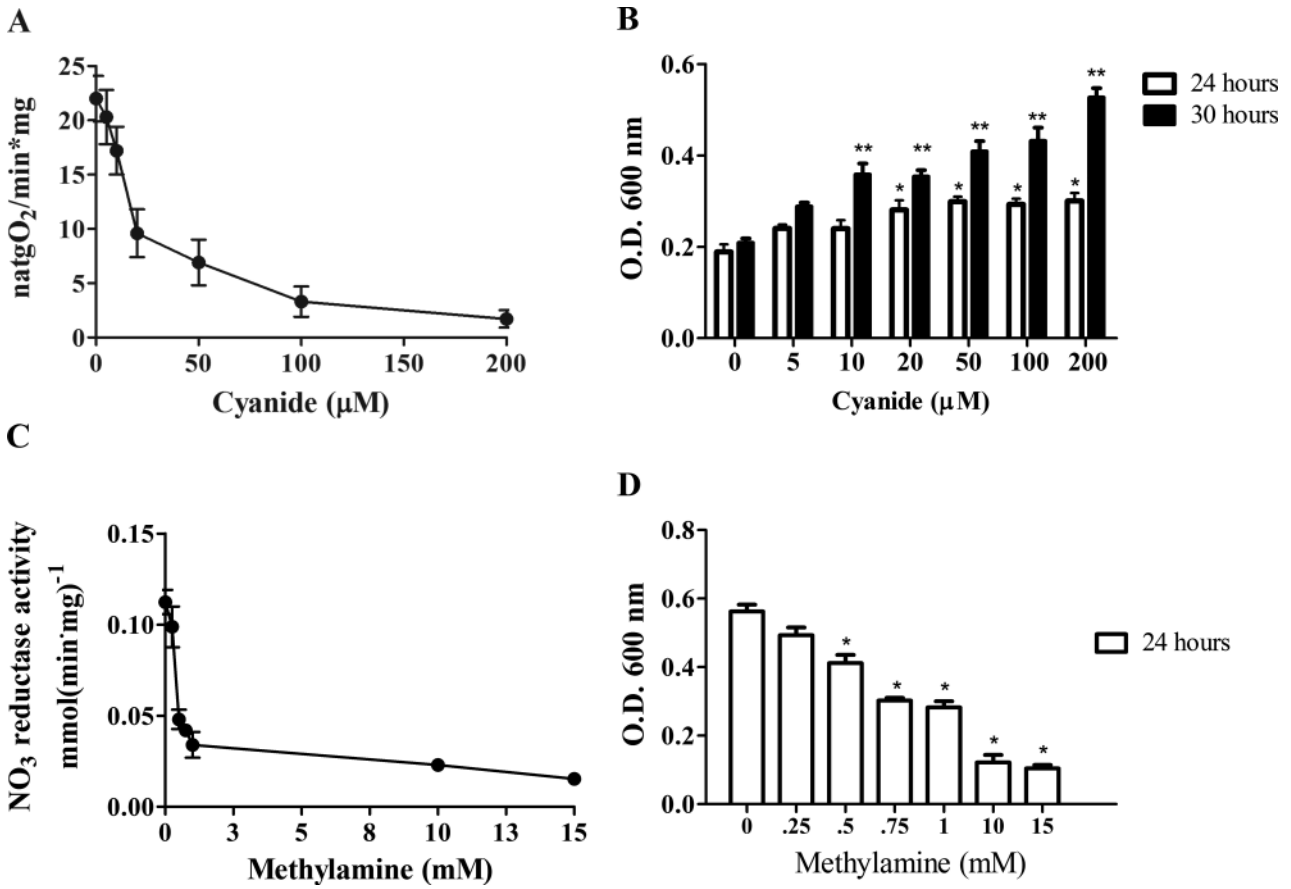

Figure 8. Effect of cyanide or methylamine on *S. epidermidis:* rate of O_2 consumption or biofilm formation. (**A**) KCN-mediated inhibition of O_2 consumption by *S. epidermidis* grown under *Ae* conditions.. Data are mean ± SD from $n = 4$. (**B**) Biofilm formation by *S. epidermidis* cultures at 24 and 30 h in *Ae* and in the presence of KCN as in A. Significance (*$P < 0.01$). (**C**) Inhibition of nitrate reductase activity by methylamine in μA- *S. epidermidis*. Data are mean ± SD from $n = 4$. (**D**) Biofilm formation in 24-h cultures grown in LB medium in μA conditions and in the presence of methylamine as in C. Significant difference (*$P < 0.01$) between 0 and 0.5 mM methylamine at 24 h of growth, $n = 6$. For oxymetry, inhibitors were added directly to the reaction mixture, while in biofilm-forming assays these were present throughout the culture.

species. Among these adaptations, most prokaryotes are able to differentially express the components in their highly branched respiratory chains developing different electron transport pathways (Anraku 1988). Different terminal oxidases are expressed in response to the availability of electron acceptors in the medium, e.g. when O_2 is available it is chosen as the preferred electron acceptor (Unden and Bongaerts 1997). In anaerobic atmospheres, respiratory chains use other final electron acceptors such as nitrate, nitrite, fumarate or DMSO, which upon reduction do not provide as much energy as O_2 (Unden and Bongaerts 1997).

In some unicellulars including *Staphylococci*, different [O_2] may trigger biofilm formation (Xu *et al.* 1998; Gomez, Hontoria and Gonzalez-Lopez 2002). Other factors affecting biofilm formation are temperature, osmolarity, pH and iron concentrations (Otto 2008). Also hydrophobic surfaces provide an anchor for bacterial association (Hall-Stoodley and Stoodley 2005). Biofilms protect cells against environmental hazards and are a source of pyogenic emboli. *Staphylococcus epidermidis* increases its biofilm-forming activity when grown under anaerobiosis, probably through the expression of exopolysaccharide PIA, teichoic acids and proteins needed for biofilm maturation (Otto 2008). Here, as [O_2] was increased, biofilm formation was inhibited. When respiratory enzymes that use oxygen as electron acceptor were inhibited with cyanide (Fig. 8A) in an effort to mimic anaerobic conditions, biofilm formation increased (Fig. 8B). In contrast, when nitrate reductase activity was inhibited by methylamine (Fig. 8C) in a μA conditions and the cell was forced to use whatever O_2 was available, biofilm formation was reduced (Fig. 8D). These data suggest that expression of different respiratory chains may be tightly related to the decision the cell makes to form biofilms.

In *Staphyloccocci*, electrons flow from different dehydrogenases to menaquinone (Gotz and Mayer 2013). Bacterial respiratory chains can contain different cytochrome *c* oxidases or quinol oxidases and oxidoreductases that are expressed depending on growth conditions. Cyt *bo* expression increases in non-fermentable sources and it decreases in fermentable sources (Escamilla *et al.* 1987); cytochrome *bd* has a high affinity for O_2 and it is induced in microaerobic conditions, meanwhile cytochrome *bo* has a lower oxygen affinity and is typically induced in high [O_2]; cytochrome aa_3 is induced in high [O_2] (Shepherd and Poole 2013). *Staphylococcus aureus* expresses cytochrome *bo,* cytochrome *aa3* (qoxABCD) and possibly a cytochrome *bd* oxidase (CydAB) (Gotz and Mayer 2013), but only cytochromes *o* and *a*- have been detected by spectrophotometry (Taber and Morrison 1964). The gene cluster encoding cytochrome *bo* oxidase has not been identified so its existence is in doubt (Hammer *et al.* 2013). *Staphylococci* lack *c*-type cytochromes such as *c*-549 and *c*-554 (Faller, Götz and Schleifer 1980; Gotz and Mayer 2013).

Using data reported here, we propose a model where the branched respiratory chain of *S. epidermidis* is modified by growth at different [O_2]. The enzymes under consideration include soluble enzymes (white circles) donating their electrons to NADH dehydrogenase type II, (NDH2) (green circle) which in turn donates electrons to menaquinone (yellow circle); other membrane dehydrogenases donating electrons to menaquinone (green circles) and terminal electron acceptors, which may be O_2 dependent (blue circles) or O_2 independent (orange circle) (Fig. 9). In aerobic grown cells (*Ae*) (Fig. 9A), menaquinone receives electrons directly from a large number of membrane dehydrogenases including glycerol-3-phosphate dehydrogenase, succinate dehydrogenase, the menaquinone oxidase complex, LDH and an NDH2, which in turn receives electrons from at least two soluble enzymes: alcohol dehydrogenase and the PDC. In mitochondria LDH and glycerol-3-phosphate dehydrogenase do not donate electrons to the respiratory chain, yet in bacteria they are membrane-bound enzymes transferring their electrons directly to ubiquinol (Barnes and Kaback 1970; Lascelles 1978; Doig *et al.* 1999; Modun and Williams 1999; Dym *et al.* 2000; Delgado *et al.* 2001; Fuller *et al.* 2011). From menaquinone, electrons are transferred to one of two terminal O_2-dependent oxidases, namely, cytochrome *bo* and cytochrome aa_3.

When [O_2] decreases in the growth medium, the composition of the *S. epidermidis* respiratory chain composition changes. In microaerobic grown cells (μA) (Fig. 9B), soluble enzymes alcohol dehydrogenase and pyruvate dehydrogenase activities remain. Among membrane dehydrogenases, glycerol 3-phosphate dehydrogenase and succinate dehydrogenase become non-detectable, while NDH2, lactate DH and the MQO complex do not seem to change. Among the final electron-acceptors, cytochrome aa_3 disappears, cytochrome *bo* decreases, and an O_2-independent nitrate reductase is expressed at low levels (Fig. 9B). In anaerobic grown cells (*An*) (Fig. 9C), dehydrogenases do not change, while cytochrome *bo* almost disappears. The most striking characteristic of the *An* cell was the high expression of nitrate reductase as the anaerobic final electron acceptor of the respiratory chain. The lack of complexes III and IV is in agreement with the notion that in *Staphylococci* electrons flow from different dehydrogenases to menaquinone and from menaquinone to different quinol oxidases, e.g. *S. epidermidis* ATCC 12228 grown in aerobic conditions contains two main cytochromes: *cyt bo* and *cyt aa3* and this is similar to the reported respiratory chain from *S. aureus* (Taber and Morrison 1964).

The spectra we obtained suggest the presence of cytochromes *aa3* and *bo*. However, the genome shown only one *qox*ABCD operon, and thus there are no genes for *bo* cytochromes. A possible explanation for our data may be that a promiscuous assembly of cytochrome *c* oxidase apo-proteins with hemes *b* and *o* occurred, where a *bo* cytochrome replaced heme *aa3*. Under specific culture conditions, bacterial oxidases may be assembled promiscuously accepting a different heme group to that present on its original structure. Examples of these substitutions have been described previously (Matsushita *et al.* 1992; Puustinen *et al.* 1992; Peschek *et al.* 1995; Sakamoto, Handa and Sone 1997; Azarkina *et al.* 1999; Contreras-Zentella *et al.* 2003). Even though we did not observe absorption bands characteristics of the cytochrome *d* at 630 nm, proteins that form the Cytochrome *d* ubiquinol oxidase are reported in the Uniprot databank (SE0785, SE 0784). The possibility that there is a similar promiscuous substitution of heme groups has to be considered. Previous reports on *Pseudomonas aeruginosa* that encodes a cyanide-insensitive oxidase (*CioAB*), which is homologous to the Cytochrome *bd* oxidase (*CydAB*) of *E. coli*, indicate that there is a substitution of *b*-type cytochromes instead of *d*-type cytochromes and this prevents the detection of an absorption peak at 630 nm (Cooper, Tavankar and Williams 2003). Furthermore, in *Campylobacter jejuni* the *cydAB* genes reported in the genome apparently encode a cyanide-resistant oxidase that does not have a *d*-type cytochrome (Jackson *et al.* 2007). The oxidoreductases we proposed (Fig. 9) were sought in the Uniprot proteome database. We did find expression of proteins exhibiting each of the activities detected here (Table 2). In addition, we found in the proteome some oxidoreductases, namely Glycerol dehydrogenase (SE0235) and Cytochrome *d* ubiquinol oxidase-like proteins I (SE0784) and II (SE0785) that were not detected in our experiments.

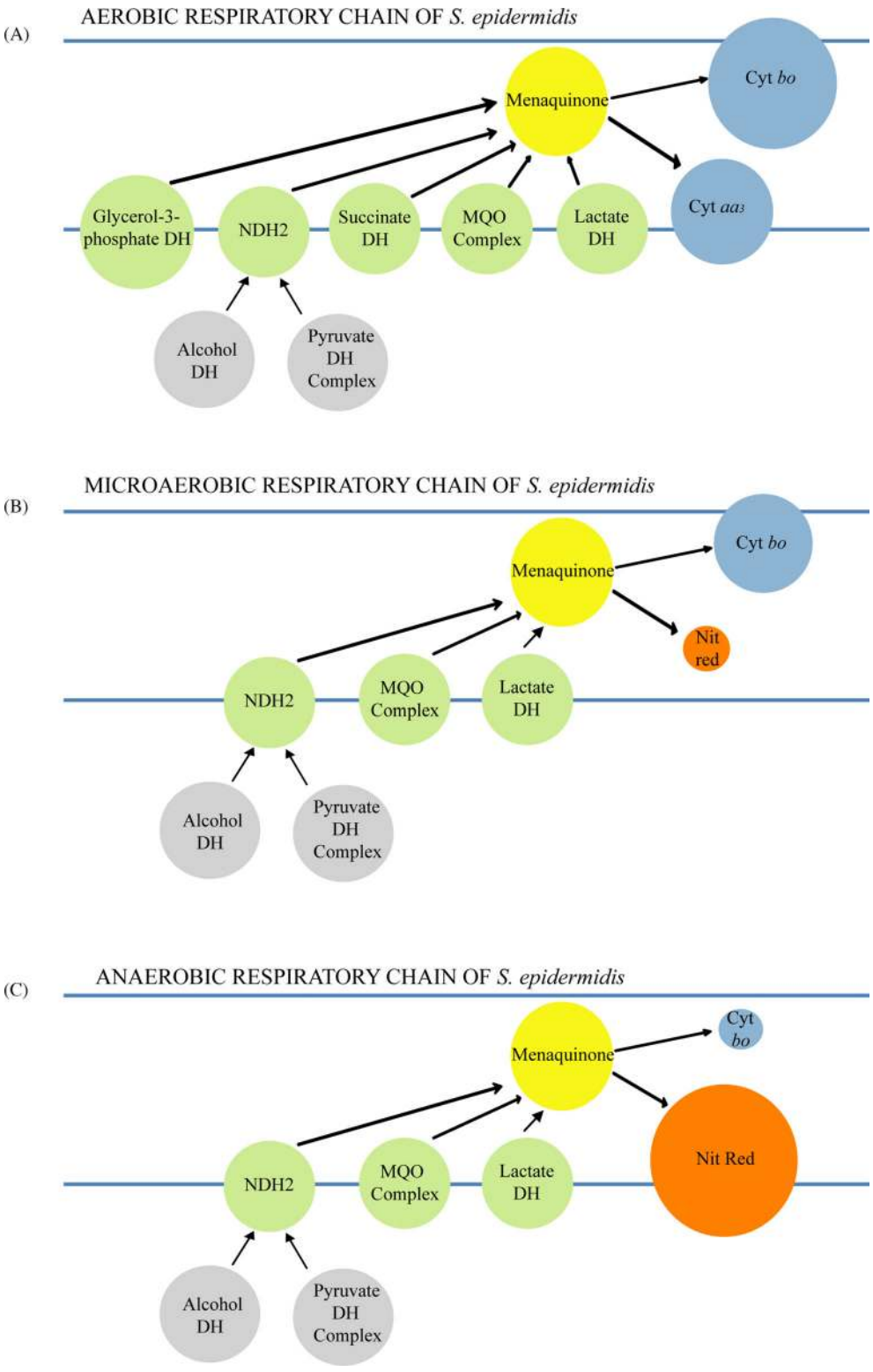

Figure 9. Proposed models of the *S. epidermidis* respiratory chain in response to [O_2] during growth. Color code: soluble enzymes (gray), membrane dehydrogenases (green); menaquinone (yellow); O_2-dependent terminal electron acceptors (blue) or O_2-independent acceptors (orange). (**A**) In aerobic (*Ae*) grown cells menaquinone receives electrons from glycerol-3-phosphate dehydrogenase, succinate dehydrogenase, the menaquinone oxidase complex, LDH or a NDH2, which receives electrons from at least two soluble enzymes: alcohol dehydrogenase and the PDC. From menaquinone, electrons are transferred to one of two terminal O_2-dependent oxidases, namely, cytochrome *bo* and Cytochrome *aa3*. (**B**) In μA, soluble enzymes (alcohol dehydrogenase and pyruvate dehydrogenase) remain. Glycerol 3-phosphate dehydrogenase and succinate dehydrogenase become non-detectable, while NDH2, lactate DH and the MQO complex do not change. Cytochrome *aa3* disappears, cytochrome *bo* decreases, and an O_2-independent nitrate reductase is expressed at low levels. (**C**) In anaerobic (*An*) conditions, dehydrogenases do not change, cytochrome *bo* almost disappears and nitrate reductase is highly expressed.

Table 2. Possible correspondence between oxidoreductase activities detected here and oxidoreductases found in the Uniprot proteome database.

Oxidoreductases found in the proteome database	Detected here by LC-MS and/or enzymatic activities	Uniprot Databank Accession number
Glycerol dehydrogenase	No	SE0235
Glyceraldehyde-3-phosphate dehydrogenase	Yes	SE0557, SE1361
NADH dehydrogenase	Yes	SE0635, SE2333
Alcohol dehydrogenase	Yes	SE0375
D,L-Lactate dehydrogenase	Yes	SE2074, SE2145
Succinate dehydrogenase	Yes	SE0841, SE0842
Succinate dehydrogenase cytochrome b-558	Yes	SE0840
Glycerol-3-phosphate dehydrogenase	Yes	SE0979
Malate dehydrogenase	Yes	SE0461
Probable quinol oxidase	Yes	SE0756, SE0757, SE0758, SE0759
Cytochrome d ubiquinol oxidase like protein	No	SE0784, SE0785
Respiratory nitrate reductase	Yes	SE1972, SE1973, SE1974, SE1975

Non-pathogenic staphylococcal species such as the ATCC12228 encode a pyocyanin- and cyanide-insensitive cytochrome *bd* quinol oxidase, while pathogenic species, such as *S. aureus* encode a sensitive variant; yet, in our hands no *bd* cytochrome was found (Voggu *et al.* 2006). Even when *S. epidermidis* was grown in a non-fermentable carbon source medium in the presence of 1 mM of KCN cytochrome *bd* was not present. The glycerol-3-phosphate dehydrogenase from *S. epidermidis* is more active than other bacteria used in biotechnology for glycerol degradation (Holmberg *et al.* 1990; Yazdani and Gonzalez 2007; da Silva, Mack and Contiero 2009). The PDC enzymes we found on membranes are usually reported as cytoplasmic enzymes, but they were also found in the membrane fraction of *Mycoplasma pneumonia* (Dallo *et al.* 2002) and Rhodospirillum *rubrum* (Luderitz and Klemme 1977).

Knowledge on how branched respiratory chains provide survival capabilities to cells can help identify specific respiratory chain inhibitors that can be used as therapeutic targets in human infections. Even though we are suggesting that the enzymes that are expressed at low oxygen concentrations may be therapeutic targets, we do not know exactly how they act during biofilm maturation. Previous studies state that anaerobic conditions increase polysaccharide gene expression in staphylococci (Cramton *et al.* 2001). Interestingly, methylamine was an effective inhibitor of the *S. epidermidis* nitrate reductase, the main final-electron acceptor present during microaerobic or anaerobic growth, and by consequence reduced biofilm formation. The high adaptability of *S. epidermidis* plays an important role in its pathogenicity and this has to be analyzed thoroughly. Already, the large effects of $[O_2]$ on biofilm formation and on the respiratory chain composition of *S. epidermidis* suggest preventive and therapeutic strategies against this bacterium.

ACKNOWLEDGEMENTS

Ramón Méndez, Martha Calahorra and Norma Sánchez provided technical assistance for this project.

FUNDING

Partially funded by grants CONACYT 239487 and UNAM-DGAPA-PAPIIT IN204015 to SUC. CUA is a CONACYT fellow enrolled in the Biochemistry PhD program at UNAM.

Conflict of interest. None declared.

REFERENCES

Anraku Y. Bacterial electron transport chains. *Annu Rev Biochem* 1988;**57**:101–32.

Artzatbanov V, Petrov VV. Branched respiratory chain in aerobically grown *Staphylococcus aureus*—oxidation of ethanol by cells and protoplasts. *Arch Microbiol* 1990;**153**:580–4.

Atkuri KR, Herzenberg LA, Niemi AK, *et al.* Importance of culturing primary lymphocytes at physiological oxygen levels. *P Natl Acad Sci USA* 2007;**104**:4547–52.

Azarkina N, Siletsky S, Borisov V, *et al.* A cytochrome bb'-type quinol oxidase in *Bacillus subtilis* strain 168. *J Biol Chem* 1999;**274**:32810–7.

Baradaran R, Berrisford JM, Minhas GS, *et al.* Crystal structure of the entire respiratory complex I. *Nature* 2013;**494**:443–8.

Barnes EM, Jr, Kaback HR. Beta-galactoside transport in bacterial membrane preparations: energy coupling via membrane-bounded D-lactic dehydrogenase. *P Natl Acad Sci USA* 1970;**66**:1190–8.

Bergsma J, Van Dongen MB, Konings WN. Purification and characterization of NADH dehydrogenase from *Bacillus subtilis*. *Eur J Biochem* 1982;**128**:151–7.

Burton RM. Glycerol dehydrogenase from Aerobacter aerogenes. In: Colowick SP, Kaplan NO (eds). *Methods in Enzymology* Vol. 1 in [59] pp. 397–400. NY: Academic Press, 1955.

Cecchini G, Schroder I, Gunsalus RP, *et al.* Succinate dehydrogenase and fumarate reductase from *Escherichia coli*. *Biochim Biophys Acta* 2002;**1553**:140–57.

Cogen AL, Yamasaki K, Sanchez KM, *et al.* Selective antimicrobial action is provided by phenol-soluble modulins derived from *Staphylococcus epidermidis*, a normal resident of the skin. *J Invest Dermatol* 2010;**130**:192–200.

Contreras-Zentella M, Mendoza G, Membrillo-Hernandez J, *et al.* A novel double heme substitution produces a functional bo3 variant of the quinol oxidase aa3 of *Bacillus cereus*. Purification and paratial characterization. *J Biol Chem* 2003;**278**:31473–8.

Cooper M, Tavankar GR, Williams HD. Regulation of expression of the cyanide-insensitive terminal oxidase in *Pseudomonas aeruginosa*. *Microbiology* 2003;**149**:1275–84.

Cotter JJ, O'Gara JP, Casey E. Rapid depletion of dissolved oxygen in 96-well microtiter plate *Staphylococcus epidermidis* biofilm assays promotes biofilm development and is influenced

by inoculum cell concentration. *Biotechnol Bioeng* 2009;**103**:1042–7.

Cotter JJ, O'Gara JP, Mack D, *et al.* Oxygen-mediated regulation of biofilm development is controlled by the alternative sigma factor sigma(B) in *Staphylococcus epidermidis*. *Appl Environ Microb* 2009;**75**:261–4.

Cramton SE, Gerke C, Schnell NF, *et al.* The intercellular adhesion (ica) locus is present in *Staphylococcus aureus* and is required for biofilm formation. *Infect Immun* 1999;**67**:5427–33.

Cramton SE, Ulrich M, Gotz F, *et al.* Anaerobic conditions induce expression of polysaccharide intercellular adhesin in *Staphylococcus aureus* and *Staphylococcus epidermidis*. *Infect Immun* 2001;**69**:4079–85.

da Silva GP, Mack M, Contiero J. Glycerol: a promising and abundant carbon source for industrial microbiology. *Biotechnol Adv* 2009;**27**:30–9.

Dallo SF, Kannan TR, Blaylock MW, *et al.* Elongation factor Tu and E1 beta subunit of pyruvate dehydrogenase complex act as fibronectin binding proteins in *Mycoplasma pneumoniae*. *Mol Microbiol* 2002;**46**:1041–51.

Delgado ML, O'Connor JE, Azorin I, *et al.* The glyceraldehyde-3-phosphate dehydrogenase polypeptides encoded by the *Saccharomyces cerevisiae* TDH1, TDH2 and TDH3 genes are also cell wall proteins. *Microbiology* 2001;**147**:411–7.

Desriac N, Broussolle V, Postollec F, *et al. Bacillus cereus* cell response upon exposure to acid environment: toward the identification of potential biomarkers. *Front Microbiol* 2013;**4**:284.

Doig P, de Jonge BL, Alm RA, *et al. Helicobacter pylori* physiology predicted from genomic comparison of two strains. *Microbiol Mol Biol R* 1999;**63**:675–707.

Dym O, Pratt EA, Ho C, *et al.* The crystal structure of D-lactate dehydrogenase, a peripheral membrane respiratory enzyme. *P Natl Acad Sci USA* 2000;**97**:9413–8.

Escamilla JE, Ramírez R, Del Arenal IP, *et al.* Expression of cytochrome oxidases in *Bacillus cereus*: effects of oxygen tension and carbon source. *J Gen Microbiol* 1987;**133**:3549–55.

Faller AH, Götz F, Schleifer KH. Cytochrome-patterns of Staphylococci and Micrococci and their taxonomic implications. Zentralblatt für Bakteriologie: I. Abt. Originale C: Allgemeine, angewandte und ökologische. *Mikrobiologie* 1980;**1**:26–39.

Fazly Bazzaz BS, Jalalzadeh M, Sanati M, *et al.* Biofilm formation by *Staphylococcus epidermidis* on foldable and rigid intraocular lenses. *Jundishapur J Microbiol* 2014;**7**:e10020.

Franco AR, Cárdenas J, Fernández E. Ammonium (methylammonium) is the co-represor of nitrate reductase in *Chlamydomonas reinhardii*. *FEBS Lett* 1984;**176**:453–6.

Frerman FE, White DC. Membrane lipid changes during formation of a functional electron transport system in *Staphylococcus aureus*. *J Bacteriol* 1967;**94**:1868–74.

Fuchs S, Pane-Farre J, Kohler C, *et al.* Anaerobic gene expression in *Staphylococcus aureus*. *J Bacteriol* 2007;**189**:4275–89.

Fuller JR, Vitko NP, Perkowski EF, *et al.* Identification of a lactate-quinone oxidoreductase in *Staphylococcus aureus* that is essential for virulence. *Front Cell Infect Microbiol* 2011;**1**:19.

Gandhi M, Chikindas ML. Listeria: a foodborne pathogen that knows how to survive. *Int J Food Microbiol* 2007;**113**:1–15.

Gates AJ, Hughes RO, Sharp SR, *et al.* Properties of the periplasmic nitrate reductases from *Paracoccus pantotrophus* and *Escherichia coli* after growth in tungsten-supplemented media. *FEMS Microbiol Lett* 2003;**220**:261–9.

Gomez MA, Hontoria E, Gonzalez-Lopez J. Effect of dissolved oxygen concentration on nitrate removal from groundwater using a denitrifying submerged filter. *J Hazard Mater* 2002;**90**:267–78.

Gordon O, Vig Slenters T, Brunetto PS, *et al.* Silver coordination polymers for prevention of implant infection: thiol interaction, impact on respiratory chain enzymes, and hydroxyl radical induction. *Antimicrob Agents Ch* 2010;**54**:4208–18.

Gotz F, Mayer S. Both terminal oxidases contribute to fitness and virulence during organ-specific *Staphylococcus aureus* colonization. *MBio* 2013;**4**:e00976–13.

Gristina AG. Biomaterial-centered infection: microbial adhesion versus tissue integration. *Science* 1987;**237**:1588–95.

Guerrero-Castillo S, Vazquez-Acevedo M, Gonzalez-Halphen D, *et al.* In *Yarrowia lipolytica* mitochondria, the alternative NADH dehydrogenase interacts specifically with the cytochrome complexes of the classic respiratory pathway. *Biochim Biophys Acta* 2009;**1787**:75–85.

Haddock BA, Jones CW. Bacterial respiration. *Bacteriol Rev* 1977;**41**:47–99.

Hall-Stoodley L, Stoodley P. Biofilm formation and dispersal and the transmission of human pathogens. *Trends Microbiol* 2005;**13**:7–10.

Hammer ND, Reniere ML, Cassat JE, *et al.* Two heme-dependent terminal oxidases power *Staphylococcus aureus* organ-specific colonization of the vertebrate host. *MBio* 2013;**4**:8873–94.

Hammes-Schiffer S, Benkovic SJ. Relating protein motion to catalysis. *Annu Rev Biochem* 2006;**75**:519–41.

Hanson RS, Srinivasan VR, Halvorson HO. Biochemistry of sporulation. I. Metabolism of acetate by vegetative and sporulating cells. *J Bacteriol* 1963;**85**:451–60.

Hederstedt L. Cytochrome b reducible by succinate in an isolated succinate dehydrogenase-cytochrome b complex from *Bacillus subtilis* membranes. *J Bacteriol* 1980;**144**:933–40.

Hederstedt L. Molecular properties, genetics, and biosynthesis of *Bacillus subtilis* succinate dehydrogenase complex. *Methods Enzymol* 1986;**126**:399–414.

Holmberg C, Beijer L, Rutberg B, *et al.* Glycerol catabolism in *Bacillus subtilis*: nucleotide sequence of the genes encoding glycerol kinase (glpK) and glycerol-3-phosphate dehydrogenase (glpD). *J Gen Microbiol* 1990;**136**:2367–75.

Hurdle JG, O'Neill AJ, Chopra I, *et al.* Targeting bacterial membrane function: an underexploited mechanism for treating persistent infections. *Nat Rev Microbiol* 2011;**9**:62–75.

Jackson RJ, Elvers KT, Lee LJ, *et al.* Oxygen reactivity of both respiratory oxidases in *Campylobacter jejuni*: the cydAB genes encode a cyanide-resistant, low-affinity oxidase that is not of the cytochrome bd type. *J Bacteriol* 2007;**189**:1604–15.

Jacobs NJ, Conti SF. Effect of hemin on the formation of the cytochrome system of anaerobically grown *Staphylococcus epidermidis*. *J Bacteriol* 1965;**89**:675–9.

Kern M, Simon J. Periplasmic nitrate reduction in *Wolinella succinogenes*: cytoplasmic NapF facilitates NapA maturation and requires the menaquinol dehydrogenase NapH for membrane attachment. *Microbiology* 2009;**155**:2784–94.

Kim JH, Haff RP, Faria NC, *et al.* Targeting the mitochondrial respiratory chain of Cryptococcus through antifungal chemosensitization: a model for control of non-fermentative pathogens. *Molecules* 2013;**18**:8873–94.

Kostakioti M, Hadjifrangiskou M, Hultgren SJ. Bacterial biofilms: development, dispersal, and therapeutic strategies in the dawn of the postantibiotic era. *Cold Spring Harb Perspect Med* 2013;**3**:a010306.

Kucera I, Dadak V, Dobry R. The distribution of redox equivalents in the anaerobic respiratory chain of Paracoccus denitrificans. *Eur J Biochem* 1983;**130**:359–64.

Lancaster CR, Kroger A. Succinate: quinone oxidoreductases: new insights from X-ray crystal structures. *Biochim Biophys Acta* 2000;**1459**:422–31.

Lascelles J. sn-Glycerol-3-phosphate dehydrogenase and its interaction with nitrate reductase in wild-type and hem mutant strains of *Staphylococcus aureus*. *J Bacteriol* 1978;**133**:621–5.

Löw H, Vallin I. Succinate-linked Diphosphopyridine nucleotide reduction in Submitochondrial particles. *Biochim Biophys Acta* 1963;**69**:361–74.

Luderitz R, Klemme JH. Isolation and characterization of a membrane-bound pyruvate dehydrogenase complex from the phototrophic bacterium *Rhodospirillum rubrum* (author's transl). *Z Naturforsch C* 1977;**32**:351–61.

McCarty GW, Bremner JM. Inhibition of assimilatory nitrate reductase activity in soil by glutamine and ammonium analogs. *P Natl Acad Sci USA* 1992;**89**:5834–6.

Mack D, Davies AP, Harris LG, *et al*. Biomaterials associated infection. In: Fintan Moriarty SAJZT, Busscher HJ (eds). *Immunological Aspects and Antimicrobial Strategies. Chapter 2. Staphylococcus Epidermidis in Biomaterial-Associated Infections*. New York: Springer, 2013, 25–56.

Magalon A, Rothery RA, Lemesle-Meunier D, *et al*. Inhibitor binding within the NarI subunit (cytochrome bnr) of *Escherichia coli* nitrate reductase A. *J Biol Chem* 1998;**273**:10851–6.

Matsushita K, Ebisuya H, Ameyama M, *et al*. Change of the terminal oxidase from cytochrome a1 in shaking cultures to cytochrome o in static cultures of *Acetobacter aceti*. *J Bacteriol* 1992;**174**:122–9.

Meunier B, Madgwick SA, Reil E, *et al*. New inhibitors of the quinol oxidation sites of bacterial cytochromes bo and bd. *Biochemistry* 1995;**34**:1076–83.

Modun B, Williams P. The staphylococcal transferrin-binding protein is a cell wall glyceraldehyde-3-phosphate dehydrogenase. *Infect Immun* 1999;**67**:1086–92.

Moreno-Vivian C, Cabello P, Martinez-Luque M, *et al*. Prokaryotic nitrate reduction: molecular properties and functional distinction among bacterial nitrate reductases. *J Bacteriol* 1999;**181**:6573–84.

Morgan DJ, Sazanov LA. Three-dimensional structure of respiratory complex I from *Escherichia coli* in ice in the presence of nucleotides. *Biochim Biophys Acta* 2008;**1777**:711–8.

Mukhopadhyay R, Rosen BP, Phung LT, *et al*. Microbial arsenic: from geocycles to genes and enzymes. *FEMS Microbiol Rev* 2002;**26**:311–25.

Nakano MM, Dailly YP, Zuber P, *et al*. Characterization of anaerobic fermentative growth of *Bacillus subtilis*: identification of fermentation end products and genes required for growth. *J Bacteriol* 1997;**179**:6749–55.

Niebisch A, Bott M. Purification of a cytochrome bc-aa3 supercomplex with quinol oxidase activity from *Corynebacterium glutamicum*. Identification of a fourth subunity of cytochrome aa3 oxidase and mutational analysis of diheme cytochrome c1. *J Biol Chem* 2003;**278**:4339–46.

Okajima Y, Kobayakawa S, Tsuji A, *et al*. Biofilm formation by *Staphylococcus epidermidis* on intraocular lens material. *Invest Ophthalmol Vis Sci* 2006;**47**:2971–5.

Otto M. Staphylococcal biofilms. *Curr Top Microbiol Immunol* 2008;**322**:207–28.

Otto M. *Staphylococcus epidermidis*–the 'accidental' pathogen. *Nat Rev Microbiol* 2009;**7**:555–67.

Padgaonkar VA, Nadkarni GB. Effect of heavy water on structure-function relationship of lactate dehydrogenase from *Lactobacillus casei*. *Indian J Biochem Biophys* 1980;**17**:272–5.

Peschek GA, Alge D, Fromwald S, *et al*. Transient accumulation of heme O (cytochrome o) in the cytoplasmic membrane of semi-anaerobic *Anacystis nidulans*. Evidence for oxygenase-catalyzed heme O/A transformation. *J Biol Chem* 1995;**270**:27937–41.

Peyssonnaux C, Boutin AT, Zinkernagel AS, *et al*. Critical role of HIF-1alpha in keratinocyte defense against bacterial infection. *J Invest Dermatol* 2008;**128**:1964–8.

Puustinen A, Morgan JE, Verkhovsky M, *et al*. The low-spin heme site of cytochrome o from *Escherichia coli* is promiscuous with respect to heme type. *Biochemistry* 1992;**31**:10363–9.

Raad I, Alrahwan A, Rolston K. *Staphylococcus epidermidis*: emerging resistance and need for alternative agents. *Clin Infect Dis* 1998;**26**:1182–7.

Sakamoto J, Handa Y, Sone N. A novel cytochrome b(o/a)3-type oxidase from *Bacillus stearothermophilus* catalyzes cytochrome c-551 oxidation. *J Biochem* 1997;**122**:764–71.

Schagger H, von Jagow G. Blue native electrophoresis for isolation of membrane protein complexes in enzymatically active form. *Anal Biochem* 1991;**199**:223–31.

Schryvers A, Lohmeier E, Weiner JH. Chemical and functional properties of the native and reconstituted forms of the membrane-bound, aerobic glycerol-3-phosphate dehydrogenase of *Escherichia coli*. *J Biol Chem* 1978;**253**:783–8.

Schurig-Briccio LA, Yano T, Rubin H, *et al*. Characterization of the type 2 NADH: menaquinone oxidoreductases from *Staphylococcus aureus* and the bactericidal action of phenothiazines. *Biochim Biophys Acta* 2014;**1837**:954–63.

Shepherd M, Poole RK. Bacterial respiratory chains. In: Roberts GCK (ed.). *Encyclopedia of Biophysics*. European Biophysical Societies' Association (EBSA). Berlin, Heidelberg: Springer-Verlag, 2013, DOI: 10.1007/978-3-642-16712-6.

Sousa PM, Videira MA, Santos FA, *et al*. The bc:caa3 supercomplexes from the Gram positive bacterium *Bacillus subtilis* respiratory chain: a megacomplex organization? *Arch Biochem Biophys* 2013;**537**:153–60.

Taber HW, Morrison M. Electron transport in Staphylococci. properties of a particle preparation from exponential phase *Staphylococcus aureus*. *Arch Biochem Biophys* 1964;**105**:367–79.

Thomas JC, Vargas MR, Miragaia M, *et al*. Improved multilocus sequence typing scheme for *Staphylococcus epidermidis*. *J Clin Microbiol* 2007;**45**:616–9.

Unden G, Bongaerts J. Alternative respiratory pathways of *Escherichia coli*: energetics and transcriptional regulation in response to electron acceptors. *Biochim Biophys Acta* 1997;**1320**:217–34.

Van Eys J, Nuenke BJ, Patterson MK, Jr. The nonprotein component of alpha-glycerophosphate dehydrogenase. Physical and chemical properties of the crystalline rabbit muscle enzyme. *J Biol Chem* 1959;**234**:2308–13.

Voggu L, Schlag S, Biswas R, *et al*. Microevolution of cytochrome bd oxidase in Staphylococci and its implication in resistance to respiratory toxins released by Pseudomonas. *J Bacteriol* 2006;**188**:8079–86.

von Eiff C, Peters G, Heilmann C. Pathogenesis of infections due to coagulase-negative staphylococci. *Lancet Infect Dis* 2002;**2**:677–85.

Vuong C, Otto M. *Staphylococcus epidermidis* infections. *Microbes Infect* 2002;**4**:481–9.

Wang XM, Noble L, Kreiswirth BN, *et al*. Evaluation of a multilocus sequence typing system for *Staphylococcus epidermidis*. *J Med Microbiol* 2003;**52**:989–98.

Wessels HJ, Vogel RO, Lightowlers RN, *et al.* Analysis of 953 human proteins from a mitochondrial HEK293 fraction by complexome profiling. *PLoS One* 2013;**8**:e68340.

Wiese M, Gerlach RG, Popp I, *et al.* Hypoxia-mediated impairment of the mitochondrial respiratory chain inhibits the bactericidal activity of macrophages. *Infect Immun* 2012;**80**:1455–66.

Wittig I, Braun HP, Schagger H. Blue native PAGE. *Nat Protoc* 2006;**1**:418–28.

Wittig I, Karas M, Schagger H. High resolution clear native electrophoresis for in-gel functional assays and fluorescence studies of membrane protein complexes. *Mol Cell Proteomics* 2007;**6**:1215–25.

Wittig I, Schagger H. Advantages and limitations of clear-native PAGE. *Proteomics* 2005;**5**:4338–46.

Xu KD, Stewart PS, Xia F, *et al.* Spatial physiological heterogeneity in *Pseudomonas aeruginosa* biofilm is determined by oxygen availability. *Appl Environ Microb* 1998;**64**:4035–9.

Yazdani SS, Gonzalez R. Anaerobic fermentation of glycerol: a path to economic viability for the biofuels industry. *Curr Opin Biotechnol* 2007;**18**:213–9.

Yeh JI, Chinte U, Du S. Structure of glycerol-3-phosphate dehydrogenase, an essential monotopic membrane enzyme involved in respiration and metabolism. *P Natl Acad Sci USA* 2008;**105**:3280–5.

Young IG, Jaworowski A, Poulis MI. Amplification of the respiratory NADH dehydrogenase of *Escherichia coli* by gene cloning. *Gene* 1978;**4**:25–36.

Zimmerli W, Trampuz A, Ochsner PE. Prosthetic-joint infections. *N Engl J Med* 2004;**351**:1645–54.